IEEE Photonics Journal
An IEEE Photonics Society Publication

Enhanced Sensitivity of Silicon-On-Insulator Surface Plasmon Interferometer With Additional Silicon Layer

Volume 3, Number 3, June 2011

Khai Q. Le
Peter Bienstman

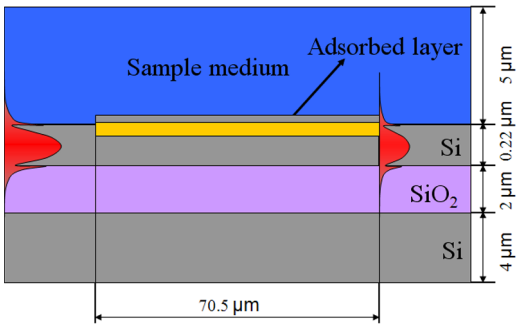

DOI: 10.1109/JPHOT.2011.2156778
1943-0655/$26.00 ©2011 IEEE

IEEE photonics SOCIETY
IEEE

Enhanced Sensitivity of Silicon-On-Insulator Surface Plasmon Interferometer With Additional Silicon Layer

Khai Q. Le and Peter Bienstman

Photonics Research Group, Department of Information Technology, Ghent University-IMEC, B-9000 Ghent, Belgium

DOI: 10.1109/JPHOT.2011.2156778
1943-0655/$26.00 ©2011 IEEE

Manuscript received February 17, 2011; revised May 9, 2011; accepted May 12, 2011. Date of publication May 19, 2011; date of current version June 14, 2011. Parts of this work were performed within the context of the Belgian IAP project Photonics@Be. Corresponding author: K. Q. Le (e-mail: khai.le@intec.ugent.be).

Abstract: It is theoretically found that by adding a thin silicon layer (35 nm) on top of our previously proposed surface plasmon interference (SPI) biosensor in silicon on insulator (SOI), a sensitivity enhancement of up to 2500 nm/refractive index units (RIUs) for short sensors can be obtained. At the same time, the corresponding figure of merit (FOM) is as high as 237 (RIU^{-1}). This improvement is caused by the reduction in group index difference between the two interfering modes.

Index Terms: Surface plasmon interferometer, silicon-on-insulator biosensors.

1. Introduction

Surface plasmon resonance (SPR) sensors, which use surface plasmon polariton (SPP) waves to probe interactions between biomolecules and sensor surfaces, have attracted tremendous interest over the past decade for optical detection of small biological or chemical entities in the kilodalton range in liquids [1]. The concept of the SPP wave is well known as the perpendicularly confined electromagnetic wave, which propagates along an interface between a metal and a dielectric.

In general, conventional SPR sensors have been restricted to the Kretschmann configuration where a thin metal film is coated on one side of the prism which separates the sensing medium and the prism. Unfortunately, the conventional configuration is not suitable for the integration into optical circuits, because of the bulk structure of a prism coated with a thin metal [2]. To integrate the traditional sensor into optical circuits, input/output parts have to be replaced with optical waveguides. Recent progress in sensitive fiber and waveguide SPR provide options for miniaturization and integration of SPR sensor systems [2]. However, the integration of fiber-SPR to other biosensor components raises some design issues. Among those include the high-precision requirement for the insertion of the fiber into a planar substrate containing fluidic circuit and chambers and the requirement of additional optical components to achieve efficient coupling of light in and out of the fiber. The proposed alternative approach to fiber-based SPR has been the planar optical waveguide structure.

Recently, we have proposed a highly integrated and sensitive SPR interferometer sensor based on silicon-on-insulator (SOI) technology [3], [4]. The basic element of the sensor is a surface plasmon based modal interferometer consisting of a thin layer of gold embedded in a

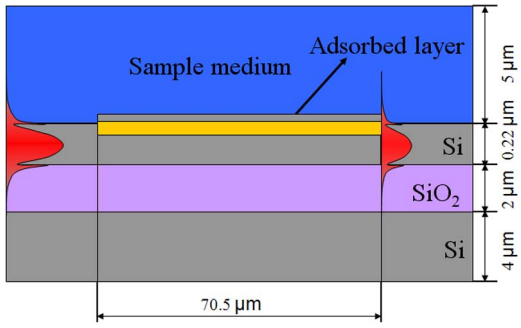

Fig. 1. Cross section of the SPI sensor on SOI with a 40-nm-thick adsorbed layer.

silicon slab. Surface modes propagate both at the gold–analyte interface (the sensing arm) and at the gold–silicon interface (the reference arm), and they recombine and interfere at the end of the gold layer. It was demonstrated that the device could achieve a sensitivity of 463.5 nm/refractive index units (RIUs) and a resolution of 1×10^{-6} RIU with regard to wavelength interrogation [3]. The refractive index of the sensed sample is 1.33. However, the sensitivity of the sensor is relatively low, and thus, an improvement to be competitive to the-state-of-the-art devices is needed.

In this paper, we found that an enhanced sensitivity of the surface plasmon interference (SPI) sensor can be obtained by adding a silicon layer on top of the Au layer.

2. Device Structure and Sensing Principle

The cross section of the SPI sensor is depicted in Fig. 1. It consists of three sections. The first and third sections are input and output dielectric waveguides, respectively, connected to a light source and a photodetector. The second section with a length L_{SPI} plays a role of surface plasmon interferometer where the sensing area is established. The interferometer consists of a thin gold (Au) layer embedded into the silicon membrane (with refractive index $n = 3.4764$) on top of a supporting silica (SiO_2) layer $(n = 1.444)$. The difference with our previous structure is the extra deposited Si layer on top of the Au layer.

When TM polarized light arrives at the beginning of the gold layer, it excites two independently propagating surface plasmon modes, which propagate along the top and the bottom interface of the metallic layer. Even though it is covered by a thin Si layer, the phase of the top surface plasmon mode is still influenced by the refractive index of the analyte medium flowing over the sensor. In contrast, the phase of the bottom surface plasmon mode is insensitive to any refractive index changes. At the end of the gold layer, both surface plasmon modes excite the ground mode of the SOI waveguide, and depending on the relative phase of the surface plasmon modes, their contributions to the ground mode will interfere constructively or destructively.

For example, the interferometric nature of the sensor is shown in Fig. 2, calculated by an in-house-developed eigenmode expansion solver [5]. This method is a full wave method which takes mode coupling and scattering correctly into account. In the simulation, the refractive index of Au is described by the Lorentz–Drude model [6]. The transmitted intensity of the fundamental TM mode of the Si slab waveguide is plotted as a function of refractive index of the sensed sample. The operation wavelength is set to 1.55 μm, which is a wavelength that achieves a suitable compromise in between the transmission properties of Si and the absorption of water. When the upper and lower surface plasmon modes arrive in phase at the end of the sensing section of length 70.5 μm, constructive interference leads to maximal transmission, whereas for certain values of the refractive index of the sample, the phase difference between the two modes results in destructive interference, leading to minima in the transmission spectrum.

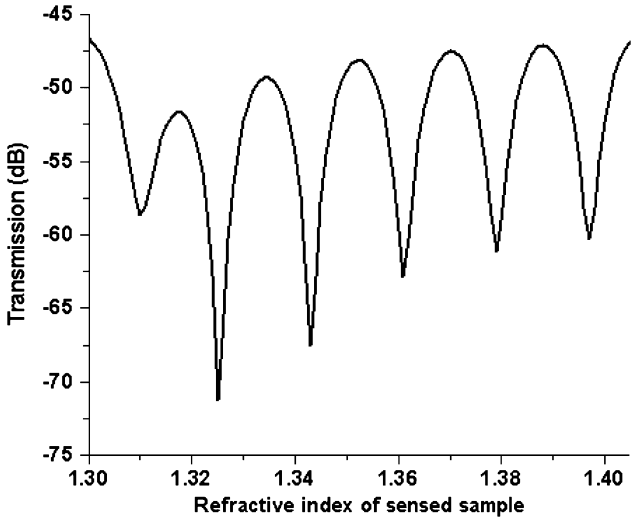

Fig. 2. Transmission of the sensor depicted in Fig. 1 as a function of refractive index of sensed sample.

Besides the intensity measurement mode [3], where we use a monochromatic input mode (at a fixed wavelength) and monitor the output power as a function of the refractive index of the sample, there also exists the so-called wavelength interrogation mode in this device, where a broadband input mode is used, and as a function of the refractive index of the sample, we monitor position of spectral minima in the transmission spectrum. Therefore, our device can operate in two modes.

3. Enhanced Sensitivity by Additional Si Top Layer

Using an adsorbed layer to enhance the sensitivity of biosensors was already proposed by Lahav *et al.* [7] to reach a sensitivity enhancement by a factor up to 10, compared with the original SPR sensor based on Kretschmann configuration. There, the enhancement is due to the evanescent field enhancement near the top layer-analyte interface. In addition, an adsorbed layer can cause the shift in plasmon resonance in plasmonic structures, which may affect the sensitivity enhancement of nanoparticle based sensors [8]. In this paper, we investigate how a thin adsorbed layer embedded on top of Au layer influences on the sensitivity of the interferometric sensor.

The bulk sensitivity of an interferometer with spectral interrogation is defined as [9]

$$S_n = \frac{\delta\lambda_{\text{res}}}{\delta n_{\text{analyte}}} \tag{1}$$

where $\delta\lambda_{\text{res}}$ is a shift in the resonance wavelength corresponding to the change $\delta n_{\text{analyte}}$ in the refractive index of analyte.

Apart from the sensitivity, another important parameter that determines performance of sensors is the Q-factor. It determines how precisely $\delta\lambda_{\text{res}}$ can be measured. The higher Q value, the more accuracy we obtain in the measurement of $\delta\lambda_{\text{res}}$. The Q-factor is defined as

$$Q = \frac{\lambda_{\text{res}}}{\text{FWHM}} \tag{2}$$

where FWHM is the full-width at half-maximum power.

To compare an overall performance of our sensors, we use the concept of a "figure of merit" (FOM). The higher FOM value, the better the sensor performance that is obtained. A typical FOM for these sensors is the ratio of the sensitivity and FWHM given as follows [10]:

$$\text{FOM} = \frac{S_n}{\text{FWHM}} \tag{3}$$

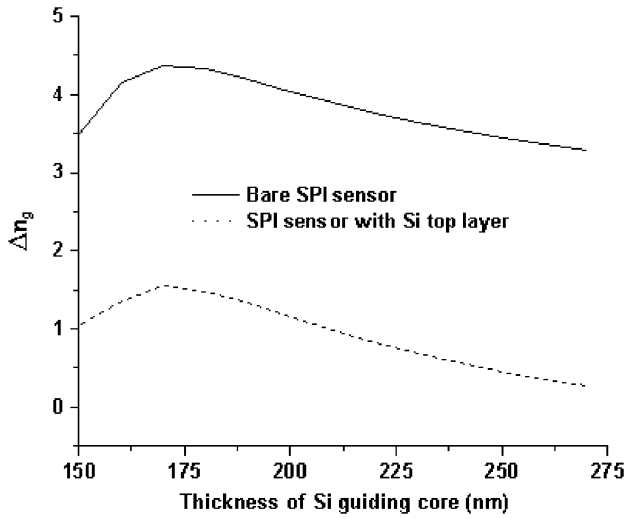

Fig. 3. Difference of top and bottom surface plasmon modes' group indices of the interferometer with respect to thickness of Si membrane.

Under the constraint of a constant phase difference the sensitivity can be written as

$$S_n = \frac{\partial\Phi(\lambda, n_{\text{analyte}})/\partial n_{\text{analyte}}}{\partial\Phi(\lambda, n_{\text{analyte}})/\partial\lambda} \tag{4}$$

with

$$\frac{\partial\Phi(\lambda, n_{\text{analyte}})}{\partial\lambda} = \frac{2\pi L_{\text{SPI}}}{\lambda}(n_{g,s} - n_{g,r}) \tag{5}$$

where $n_{g,s}$ and $n_{g,r}$ is the group indices of the sensing and reference waveguides.

This sensitivity is strongly dependent on the group index difference of the top and bottom SP modes of the interferometer. As the difference between the group indices (Δn_g) becomes smaller, the sensitivity becomes substantially larger. To improve the sensitivity, one of the best options is making the two modes more alike, which can be accomplished by adding a thin Si layer on top of the Au layer. It can be seen in Fig. 3 that the difference between the group indices of the two modes is smaller than those of our previous sensor.

To specify the improved sensitivity of the sensor and to demonstrate the best material added on the top to be Si, we calculate the sensitivity with respect to various refractive indices of the additional top layer. The first structure we investigate has a 70-nm-thick Au layer embedded into a 220-nm-thick silicon membrane with 70.5-μm-length sensed area. By changing the refractive index of the 40-nm-thick additional top layer, we monitor a shift of transmission minima in the transmission spectra to calculate the sensitivity of the sensor. We found that the highest sensitivity is 5750 nm/RIU with a corresponding refractive index of the additional top layer of 3.476, as seen in Fig. 4. This index is the one of Si, again giving evidence for the theory that making the interferometer more symmetrical is the reason for the improvement. The corresponding Q-factor and FOM of the new sensor are 105 and 383 (RIU^{-1}), and that of the old one is 171 and 56 (RIU^{-1}), respectively. It is seen that the overall performance of the new sensor is better than the old one.

However, since the length of the sensor is relatively long, it is not suitable for densely integrated on-chip applications where the size of the sensor is required to be as small as possible. We now turn to optimize the device to obtain a small sensor with high selectivity and sensitivity. The optimization of the sensor is to determine the suitable values of the thickness of Si guiding core (d_{core}), the length of the sensing area (L_{SPI}), and the thickness of the Au and Si top layer. The selection of

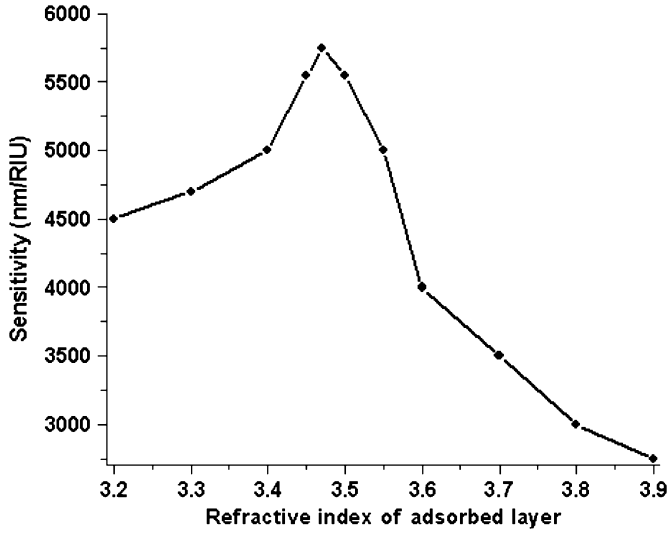

Fig. 4. Sensitivity of the sensor with respect to refractive index of additional adsorbed layer.

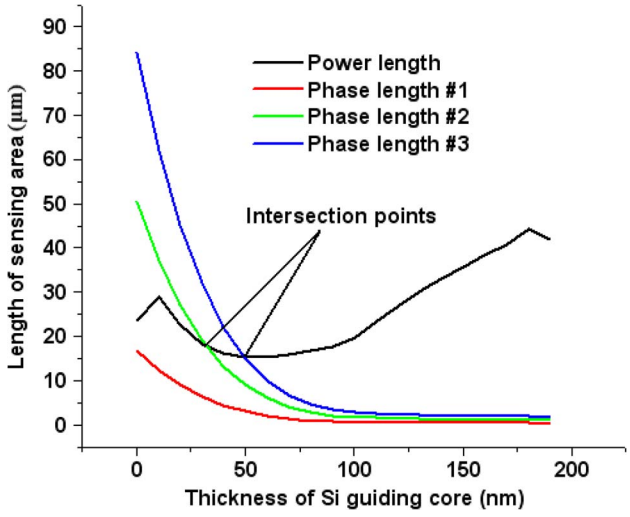

Fig. 5. Phase lengths and power length of the sensor as a function of thickness of Si waveguide core. The thickness of Au and Si top layer is 60 nm and 35 nm, respectively.

those parameters is done so that the transmission of the sensor reaches its minimum at a wavelength of 1.55 μm. The minimum appears when the interference of two plasmon modes is totally destructive and when both modes carry the same amount of power. This leads to the fact that the optimal length of the sensor has to satisfy the two following equations [9]:

$$2(\phi_{b0} - \phi_{t0}) - \left(k_r^{b0} - k_r^{t0}\right) L_{SPI} = (2m+1)\pi \tag{6}$$

$$L_{SPI} = \frac{1}{k_i^{t0} - k_i^{b0}} \ln\left(\frac{|T_{b0}|^2}{|T_{t0}|^2}\right) \tag{7}$$

where ϕ_{b0} and ϕ_{t0} are the phase difference due to the coupling of the incoming silicon waveguide mode to the bottom SP mode and the top SP mode, respectively. T_{b0} and T_{t0} are the transmission coefficients of the incoming dielectric mode to the bottom and the top SP modes at the chosen

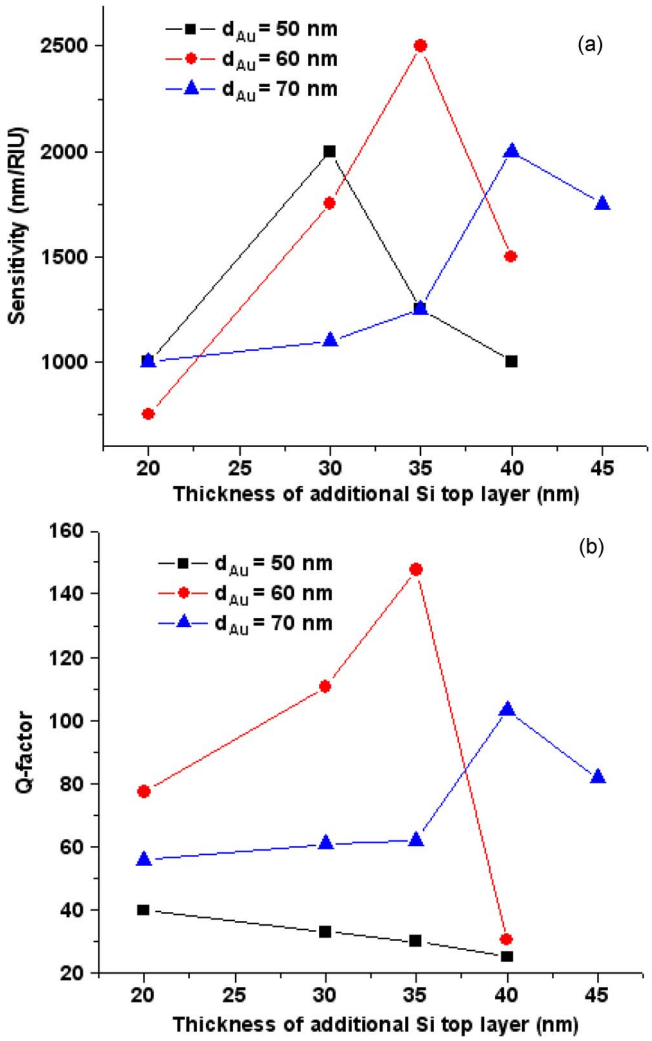

Fig. 6. Sensitivity (a) and *Q*-factor (b) as a function of thickness of Si top layer with various Au layer thicknesses, each time for the optimal core thickness and sensor length.

wavelength or refractive index for which the transmission should be minimal, and k_r^{b0}, k_i^{b0}, k_r^{t0}, and k_i^{t0} are the real and imaginary parts of the *k*-vector of the bottom and top SP modes, respectively.

Equation (6) provides us various possible phase lengths corresponding to the order of the interference effect with $m = 0, 1, 2 \ldots$, and (7) only gives us one single possible power length. The intersection of phase lengths and power length results in optimal pairs $(L_{\text{SPI}}, d_{\text{core}})$ of the sensing length and the Si core thickness. For example, with a given thickness of the additional Si top layer and Au layer, the phase lengths and the power length with respect to the sensing length and the Si core thickness are depicted in Fig. 5. Since there exist various optimal pairs $(L_{\text{SPI}}, d_{\text{core}})$, the most optimal one is chosen so that the highest sensitivity and *Q*-factor is obtained.

Following design rules, we are seeking the most optimal pairs $(L_{\text{SPI}}, d_{\text{core}})$ of the SPI sensor with respect to thickness of the Si top layer and Au layer. Since we aim at small sensors with a length shorter than 15 μm, we only choose certain thickness of the Si top layer and Au layer. Each time for the optimal pair $(L_{\text{SPI}}, d_{\text{core}})$, the sensitivity and *Q*-factor of the sensor as a function of the thickness of Si top layer with various Au layers is depicted in Fig. 6(a) and (b), respectively. With each Au layer, the highest sensitivity is found for a given thickness of the Si top layer. It is seen that the highest sensitivity and *Q*-factor is found for a 35-nm-thick Si top layer and a 60-nm-thick Au layer. The corresponding optimal pair $(L_{\text{SPI}}, d_{\text{core}})$ of the SPI sensor is (15.02 μm, 109.6 nm). The optimal

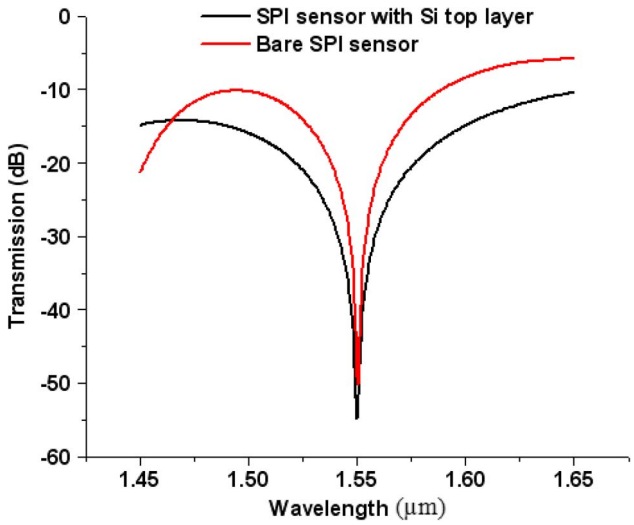

Fig. 7. Transmission as a function of wavelength. Simulation results for the most optimized structure.

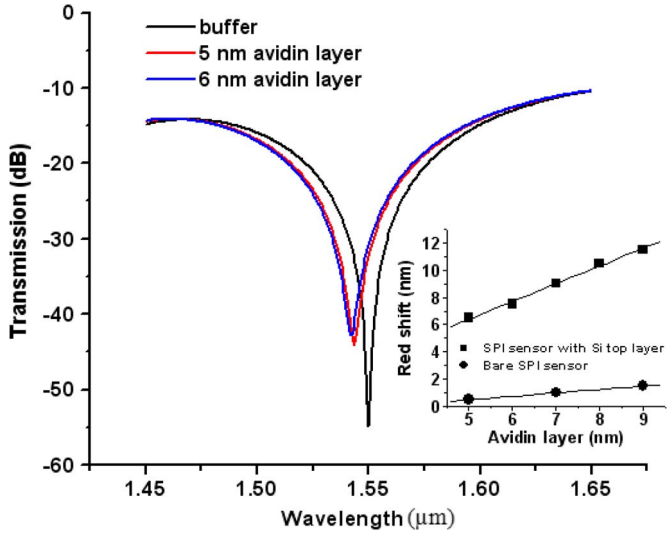

Fig. 8. Transmission of sensors as a function of wavelength. Inset is red shift for various avidin layers.

value is the result of a tradeoff between two effects; the thicker the additional Si layer, the more symmetrical the system becomes but the smaller the effect of the liquid on the phase of the top mode will be. For comparison, the most optimal pair $(L_{\mathrm{SPI}}, d_{\mathrm{core}})$ of the bare SPI sensor is found at (5.63 μm, 140.4 nm). The sensitivity of the optimized sensor with 35-nm-thick Si top layer is around 2500 nm/RIU, and that of the bare sensor is around 750 nm/RIU. The transmission spectra of the sensors as a function of wavelength are depicted in Fig. 7. The *Q*-factor of the bare sensor is around 207, while that of the sensor with Si top layer is 148. Following (3), the FOM of the bare sensor has a value of 100 (RIU^{-1}), while that of the sensor with Si top layer is 237 (RIU^{-1}). It implies that the new sensor with the most optimal pair $(L_{\mathrm{SPI}}, d_{\mathrm{core}})$ has better performance than the old one.

Apart from bulk sensing, the new configuration, which makes the interferometer more symmetrical, also helps to enhance the sensitivity of the device for surface sensing. To model surface sensing, we simulate the response when adding layers of avidin of different thickness with index 1.45

(which holds for any close packed monolayer of proteins). In reality, complete saturation of the device with avidin, when all the binding sites at the surface are occupied, will be reached for an additional 5 nm layer with refractive index of 1.45 [11]. It is found that the red shift for such a thin layer of the new sensor is 6.5 nm. That for the original one is 0.5 nm. The red shift with respect to thickness of the added avidin layer is depicted in Fig. 8. It is seen that the resonance wavelength is linearly shifted with respect to an increase of the added avidin layer.

4. Conclusion

In this paper, we have theoretically proposed the utility of the Si top layer to make the interferometer more symmetrical to enhance the sensitivity of the SPI biosensor on SOI. It is found that when the 35-nm Si layer is added on top of the 60-nm Au layer, the high sensitivity and FOM of the SPI sensor with optimal length of 15.02 μm can be obtained at 2500 nm/RIU and 237 (RIU^{-1}), respectively. The experimental demonstration of this work will be reported in future publications.

References

[1] J. Homola, S. Yee, and G. Gauglitz, "Surface plasmon resonance sensors: Review," *Sens. Actuators B, Chem.*, vol. 54, no. 1/2, pp. 3–15, Jan. 1999.
[2] X. D. Hoa, A. G. Kirk, and M. Tabrizian, "Towards integrated and sensitive surface plasmon resonance biosensors: A review of recent progress," *Biosens. Bioelectron.*, vol. 23, no. 2, pp. 151–160, Sep. 2007.
[3] P. Debackere, S. Scheerlinck, P. Bienstman, and R. Baets, "Surface plasmon interferometer in silicon-on-insulator: Novel concept for an integrated biosensor," *Opt. Exp.*, vol. 14, no. 16, pp. 7063–7072, Aug. 2006.
[4] P. Debackere, R. Baets, and P. Bienstman, "Bulk sensing experiments using a surface plasmon interferometer," *Opt. Letts.*, vol. 34, no. 18, pp. 2858–2860, Sep. 2009.
[5] CAMFR. [Online]. Available: http://camfr.sourceforge.net
[6] A. D. Rakic, A. B. Djurisic, J. M. Elazar, and M. L. Majewski, "Optical properties of metallic films for vertical-cavity optoelectronic devices," *Appl. Opt.*, vol. 37, no. 22, pp. 5271–5283, Aug. 1998.
[7] A. Lahav, M. Auslender, and I. Abdulhalim, "Sensitivity enhancement of guided-wave surface-plasmon resonance sensors," *Opt. Letts.*, vol. 33, no. 21, pp. 2539–2541, Nov. 2008.
[8] M. B. Cortie and A. M. McDonagh, "Synthesis and optical properties of hybrid and alloy plasmonic nanoparticles," *Chem. Rev.*, 2011, dx.doi.org/10.1021/cr1002529
[9] P. Debackere, "Nanophotonic biosensor based on surface plasmon interference," Ph.D. dissertation, Ghent Univ., Ghent, Belgium, 2010, pp. 4-22–4-36.
[10] L. J. Sherry, S.-H. Chang, G. C. Schatz, R. P. Van Duyne, B. J. Willey, and Y. Xia, "Localized surface plasmon resonance spectroscopy of single Silver nanocubes," *Nano Lett.*, vol. 5, no. 10, pp. 2034–2038, Oct. 2005.
[11] T. Claes, J. G. Morela, K. De Vos, E. Schacht, R. Baets, and P. Bienstman, "Label-free biosensing with a slot-waveguide-based ring resonator in silicon-on-insulator," *IEEE Photon. J.*, vol. 1, no. 3, pp. 197–204, Sep. 2009.